

Fast *ab initio* methods for the calculation of adiabatic spin wave spectra in complex systems

O. Grotheer, C. Ederer, and M. Fähnle

Max-Planck-Institut für Metallforschung, Heisenbergstrasse 1, D-70569, Stuttgart, Germany

(Received 12 September 2000; published 6 February 2001)

The interpretation of the physics of magnets with reduced dimensionality often requires information on the spin wave excitations at arbitrary wavelengths which is generally hard to obtain experimentally. Two powerful methods for the *ab initio* calculation of adiabatic spin-wave spectra are introduced, a frozen-magnon-torque method for systems with large exchange fields and a transverse-susceptibility method which may be used also for materials with smaller exchange fields. The efficiency of both methods results from the fact that the number of calculations required to obtain the spin-wave spectrum scales linearly with the number of basis atoms in the unit cell. Results are given for Fe, Co, Ni, permalloy Ni₃Fe, and CoFe, materials which are often used for thin-film technologies.

DOI: 10.1103/PhysRevB.63.100401

PACS number(s): 75.30.Ds, 71.15.Ap, 71.15.Mb

In recent years magnetism in reduced dimensionality has become extremely important because of the very rapid development of thin-film technologies for basic research and for applications in magnetotransport. Thereby, spin excitations like single-particle Stoner excitations or collective spin-wave excitations¹ play a central role for thermostatic phenomena, but also for the transport phenomena because the spin-dependence of the inelastic mean free path of an excited hot electron is determined by spin-flip exchange scattering at these excitations.^{2,3} A quantitative analysis of the various phenomena requires information about the spin-wave spectra which is often difficult to obtain experimentally. One example is the spin-dependent transport of hot electrons in a spin-valve transistor where in the “bulk” of the metallic components spin-flip exchange scattering at spin waves of all wavelengths occurs. Because the energies of short-wavelength spin waves in 3*d* transition metals are very large, it is difficult and costly to investigate the *bulk* spin wave spectra of various 3*d* magnets used in the devices by neutron-scattering experiments. A second example is the generation of magnons by hot electrons at the *interfaces* between the insulating barrier and the magnetic electrodes of magnetic tunnel junctions which is responsible for the reduction of the magnetoresistance.⁴ Because the magnon spectrum at such an interface is hardly accessible by experiments, the quantitative analysis of the data so far must manage with a simple modelling of the spin-wave spectra by a Debye model.⁴ Finally, the short-wavelength spin waves at *surfaces* or in *ultrathin magnetic films* of few magnetic monolayers contribute to the spin polarized electron energy loss spectrum.³ Whereas low-energy spin waves in ultrathin films can be studied by ferromagnetic resonance⁵ or by Brillouin scattering experiments,⁶ the direct experimental determination of the short-wavelength spectrum is again difficult.

From the above discussion it becomes obvious that a theoretical determination of spin wave spectra would be extremely helpful for a quantitative analysis of experimental data, especially for complex situations like compounds, surfaces and interfaces. Thereby, the methods of the *ab initio* electron theory have to be used to cope with the interplay between structure and exchange interactions in a self-

consistent manner which is not possible within phenomenological models like the Heisenberg model or the Hubbard Hamiltonian.¹

For a full account of the excitations in principle the dynamic transverse susceptibility $\chi_{+-}(\mathbf{q}, \omega)$ had to be calculated¹ which contains both the single-particle Stoner excitations and the spin-wave excitations as well as their interference which determines, e.g., the lifetime of the magnons. This has been achieved by Savrasov⁷ within the framework of the time-dependent *ab initio* linear-response density-functional theory, which at present, however, is too costly to be applied to complex systems. We therefore adopt the adiabatic approximation which is based on the notion that the very rapid electronic degrees of freedom can adjust almost instantaneously to the slow magnetic degrees of freedom described by the orientations of the magnetic moments, so that the electronic system is assumed to be all the time in its ground state with respect to the momentary directions of the moments. The theory of adiabatic spin-wave spectra has been developed mainly in the last five years.⁸⁻¹⁰ Because the interference of the magnons with the single-particle Stoner excitations is neglected in the adiabatic approximation, the magnon lifetimes and special features of the spectrum at shorter wavelengths arising from this interference like the “optical magnon branch” in Ni around 150 meV (Ref. 11) cannot be obtained. Altogether, the adiabatic theory represents an excellent approximation for the long-wavelength limit and a reasonable approximation for smaller wavelengths.

In the present paper we introduce two methods to calculate adiabatic spin-wave spectra by the *ab initio* density-functional theory in local-spin-density approximation (LSDA).¹² Combined with the time-saving atomic-sphere approximation for the potential and the spin direction (see below) they are able to yield a reasonably fast and semiquantitative overall description of the spin wave spectra in complex systems, e.g., at surfaces and interfaces, which is certainly superior to model descriptions like the Debye model sometimes used⁴ for complex situations. The capability of the method is demonstrated for Fe, Ni, Co, Ni₃Fe, and CoFe, materials which are frequently used in magnetoresistive devices.

Among the various existing adiabatic decoupling schemes^{8–10} we use the procedure of Halilov *et al.*⁹ which results in a classical equation of motion,¹³

$$\dot{\mathbf{M}}_\alpha = -\frac{2\mu_B}{\hbar} \mathbf{N}_\alpha = -\frac{2\mu_B}{\hbar} \frac{dE}{d\mathbf{M}_\alpha} \times \mathbf{M}_\alpha, \quad (1)$$

for the lattice site spin magnetic moment \mathbf{M}_α which is just the integral of the magnetization density $\mathbf{m}(\mathbf{r})$ over an appropriately defined cell volume around lattice site α . The quantity \mathbf{N}_α represents the torque acting on \mathbf{M}_α , and $E(\{\mathbf{M}_\alpha\})$ is the energy of the system for prescribed moment directions $\{\mathbf{M}_\alpha\}$. In the following we consider a system with translation vectors \mathbf{T} and basis vectors \mathbf{R} which describe the positions of the atoms in the unit cell. In the case of a bulk material the unit cell corresponds to the elementary unit cell. To describe systems with an interface or a surface the unit cells are large supercells containing two interfaces or containing a vacuum layer (in the case of surfaces) which are repeated periodically. We furthermore assume a ferromagnetic ground state with magnetic moments in z direction. Adopting the harmonic approximation for $E(\{\mathbf{M}_\alpha\})$, Eq. (1) yields for the spin waves $M_{\mathbf{R}+\mathbf{T}}^x + iM_{\mathbf{R}+\mathbf{T}}^y = z_{\mathbf{R}+\mathbf{T}} = u_{\mathbf{R}} e^{i(\mathbf{q}\cdot\mathbf{T} + \omega t)}$ the eigenvalue equation

$$\hbar\omega(\mathbf{q})u_{\mathbf{R}} = 2\mu_B |\mathbf{M}_{\mathbf{R}}| \sum_{\mathbf{R}'} A_{\mathbf{R}\mathbf{R}'}^\perp(\mathbf{q})u_{\mathbf{R}'}, \quad (2)$$

where the $A_{\mathbf{R}\mathbf{R}'}^\perp(\mathbf{q})$ are the Fourier transforms of the transverse coupling constants

$$A_{\mathbf{R}\mathbf{R}'}^\perp(\mathbf{T}-\mathbf{T}') = \frac{\partial^2 E}{\partial M_{\mathbf{R}+\mathbf{T}}^x \partial M_{\mathbf{R}'+\mathbf{T}'}^x} = \frac{\partial^2 E}{\partial M_{\mathbf{R}+\mathbf{T}}^y \partial M_{\mathbf{R}'+\mathbf{T}'}^y}. \quad (3)$$

For a system with N basis atoms the coupling constants $A_{\mathbf{R}\mathbf{R}'}^\perp(\mathbf{q})$ are composed of N^2 independent real parameters. We now describe two methods to calculate them by the *ab initio* electron theory.

Frozen-magnon calculations. In these calculations frozen-magnon configurations of the form $z_{\mathbf{R}+\mathbf{T}} = u_{\mathbf{R}} e^{i\mathbf{q}\cdot\mathbf{T}}$ are prescribed for various sublattices. In the original version of the frozen-magnon calculations (e.g., Ref. 9) the N^2 parameters of the coupling constants then are obtained via Eq. (3) from the energy differences of N^2 different frozen-magnon configurations. We introduce a variant of the method by noting that the torques $\mathbf{N}_{\mathbf{R}}$ acting on the magnetic moments of the sublattice \mathbf{R} originating from the frozen-magnon configurations prescribed for the sublattices \mathbf{R}' are given by

$$-N_{\mathbf{R}}^y + iN_{\mathbf{R}}^x = |\mathbf{M}_{\mathbf{R}}| \sum_{\mathbf{R}'} A_{\mathbf{R}\mathbf{R}'}^\perp(\mathbf{q})u_{\mathbf{R}'}. \quad (4)$$

A complete column of the matrix $A_{\mathbf{R}\mathbf{R}'}^\perp(\mathbf{q})$ therefore may be obtained by prescribing a frozen-magnon configuration just for one sublattice \mathbf{R}' and calculating the torques acting on the magnetic moments of all sublattices \mathbf{R} . Thus, the N^2 parameters of the coupling constants may be obtained from

just N different frozen-magnon calculations, and this renders possible to deal with complex systems, i.e., large supercells containing many basis atoms.

In principle the frozen-magnon configurations with amplitudes $u_{\mathbf{R}'}$ have to be generated within the constraint density-functional approach¹⁴ with Lagrangian parameters which have to be determined self-consistently which makes the method time consuming. To make the method more effective, we do not prescribe primarily the magnetic moment directions $\mathbf{M}_{\mathbf{R}+\mathbf{T}}/|\mathbf{M}_{\mathbf{R}+\mathbf{T}}|$ but¹⁵ the directions of the local-spin quantization axes $\mathbf{e}_{\mathbf{R}+\mathbf{T}}$ for the calculation of the exchange-correlation energy in atomic-sphere approximation (ASA),¹⁶ given in the notation of Ref. 17

$$E_{\text{xc}}^{\text{ASA}} = \sum_{\mathbf{R},\mathbf{T}} \int_{\Omega_{\mathbf{R}+\mathbf{T}}} n(r) \epsilon_{\text{xc}}(n(r), \mathbf{e}_{\mathbf{R}+\mathbf{T}} \cdot \mathbf{m}(r)) d^3r. \quad (5)$$

As a consequence of this often used ASA approximation the exchange-correlation field $\mathbf{B}_{\mathbf{R}+\mathbf{T}}^{\text{xc}}$ is parallel to $\mathbf{e}_{\mathbf{R}+\mathbf{T}}$, whereas the direction of $\mathbf{M}_{\mathbf{R}+\mathbf{T}}$ deviates by an angle $\Delta\vartheta_{\mathbf{R}+\mathbf{T}}$. The torques $\mathbf{N}_{\mathbf{R}} = (\partial E / \partial \mathbf{M}_{\mathbf{R}}) \times \mathbf{M}_{\mathbf{R}}$ then are approximated by $\tilde{\mathbf{N}}_{\mathbf{R}} = (dE/d\mathbf{e}_{\mathbf{R}}) \times \mathbf{e}_{\mathbf{R}}$ calculated according to Ref. 18, and therefore the coupling constants evaluated according to Eq. (4) are not the “true” coupling constants. Systematic errors scale like $\Delta\vartheta_{\mathbf{R}}/\vartheta \sim \omega(\mathbf{q})/\langle B_{\text{xc}} \rangle$ where ϑ is the amplitude of the frozen-magnon configuration and $\langle B_{\text{xc}} \rangle$ is an appropriately averaged exchange-correlation field. For Fe with a large exchange-correlation field we find $\Delta\vartheta/\vartheta < 10\%$ even for the largest spin-wave energies $\hbar\omega(\mathbf{q})$ whereas for Ni we find $\Delta\vartheta/\vartheta$ values of up to 46%. This makes clear that frozen-magnon-ASA calculations yield reliable adiabatic spin wave spectra only for systems with large exchange-correlation fields.

Spin wave spectra from the transverse susceptibility. Instead of prescribing a frozen-magnon configuration for the moments $\mathbf{M}_{\mathbf{R}'+\mathbf{T}}$ we now apply a spiral external field $B_{\mathbf{R}'+\mathbf{T}}^x + iB_{\mathbf{R}'+\mathbf{T}}^y = |\mathbf{B}_{\mathbf{R}'}| e^{i\mathbf{q}\cdot\mathbf{T}}$ to one sublattice (\mathbf{R}'). The field is constant within each atomic sphere. The linear response has the form of spin spirals on all sublattices \mathbf{R} ,

$$M_{\mathbf{R}}^x + iM_{\mathbf{R}}^y = \chi_{\mathbf{R}\mathbf{R}'}^\perp(\mathbf{q}) |\mathbf{B}_{\mathbf{R}'}|, \quad \chi^\perp(\mathbf{q}) = [A^\perp(\mathbf{q})]^{-1}. \quad (6)$$

A complete column of the matrix $\chi^\perp(\mathbf{q})$ therefore may be obtained by prescribing a field spiral just for one sublattice \mathbf{R}' and calculating the induced magnetic moments on all other sublattices \mathbf{R} . Thus, the N^2 real parameters which determine the susceptibility tensor $\chi^\perp(\mathbf{q})$ for each wave vector \mathbf{q} may again be obtained from just N different calculations, and the matrix $A^\perp(\mathbf{q})$ is determined by inverting $\chi^\perp(\mathbf{q})$. Because the induced magnetic moments $\mathbf{M}_{\mathbf{R}}$ are calculated self-consistently, this method also applies to materials with smaller exchange fields. To make the calculational method time saving, we again apply the ASA approximation for the spin directions. Because the choice of the spin quantization axes $\mathbf{e}_{\mathbf{R}+\mathbf{T}}$ has an influence on the directions of the induced moments, the directions of the magnetic moments and of the spin quantization axes have to be determined self-consistently. We have shown in Ref. 17 that the error in the total energy originating from the ASA approximation is

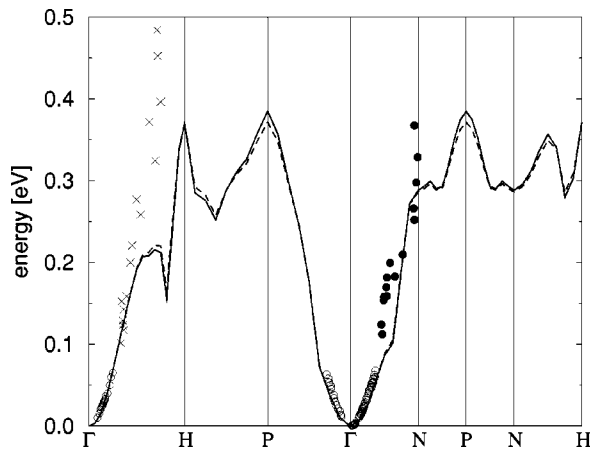


FIG. 1. Adiabatic spin-wave dispersion relations along high-symmetry lines of the Brillouin zone for Fe. Broken line: frozen-magnon-torque method, full line: transverse susceptibility method. The symbols denote results from neutron-scattering experiments: \circ (Ref. 28), \times (Ref. 29) for Fe 12% Si, \bullet (Ref. 30) for Fe 12% Si. Our results from the frozen-magnon-torque method are very similar to those of the frozen-magnon-energy method of Ref. 9.

minimized when selecting after each iteration step of this self-consistency cycle the set of spin quantization axes for the next iteration step according to $\mathbf{e}_{\mathbf{R}+\mathbf{T}} = \tilde{\mathbf{N}}_{\mathbf{R}+\mathbf{T}} / |\tilde{\mathbf{N}}_{\mathbf{R}+\mathbf{T}}|$ where the $\tilde{\mathbf{N}}_{\mathbf{R}+\mathbf{T}}$ are the torques acting on the moments after the last step. When choosing the $\mathbf{e}_{\mathbf{R}+\mathbf{T}}$ in the conventional way¹⁶ parallel to the moments after each iteration step, very large errors for $\chi^{\perp}(\mathbf{q})$ (factors 2-3) may arise.

Our calculations were performed by our recently developed version^{19,17,18} of the tight-binding linear-muffin-tin-orbital-ASA method²⁰ which is able to account for the non-collinearity of the spin configuration in the way described in Ref. 16.

The results for Fe, Co, and Ni are shown in Figs. 1, 2, and

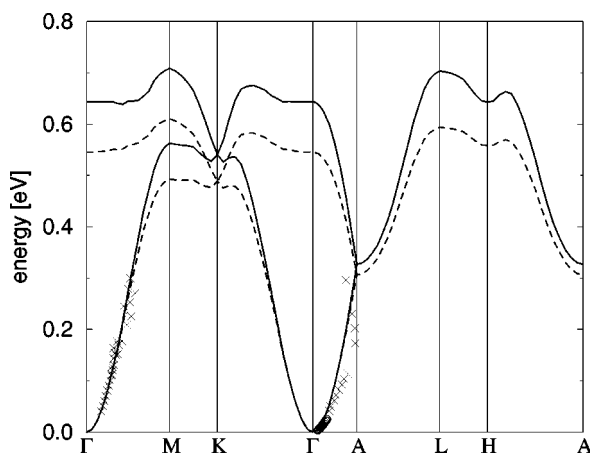


FIG. 2. Adiabatic spin-wave dispersion relations along high-symmetry lines of the Brillouin zone for Co. Broken line: frozen-magnon-torque method, full line: transverse susceptibility method. The symbols denote results from neutron-scattering experiments: \circ (Ref. 28), and \times (Ref. 31). Our results from the frozen-magnon-torque method are very similar to those of the frozen-magnon-energy method of Ref. 9.

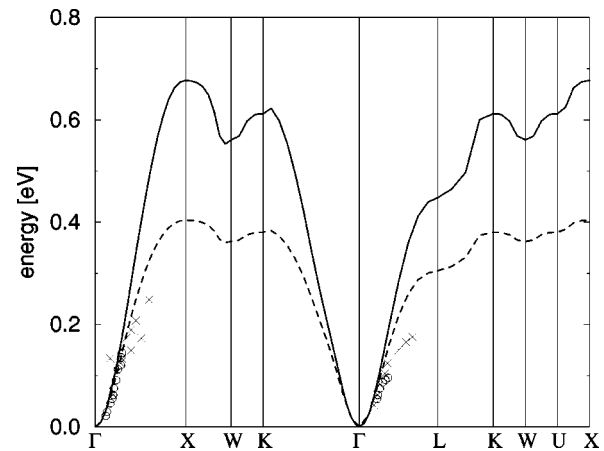


FIG. 3. Adiabatic spin-wave dispersion relations along high-symmetry lines of the Brillouin zone for Ni. Broken line: frozen-magnon-torque method, full line: transverse susceptibility method. The symbols denote results from neutron-scattering experiments: \circ (Ref. 32), and \times (Ref. 11). Our results from the frozen-magnon-torque method are similar to those of the frozen-magnon-energy method of Ref. 9 (albeit slightly larger in the high-energy regime).

3 together with experimental data. As expected, the results of the two calculational methods agree well for the case of Fe because there the angle $\Delta\vartheta$ between the actual magnetic moment direction and the direction of the spin quantization axis prescribed in the frozen-magnon method is small due to the large exchange-correlation field. In contrast, for Ni which has a much smaller exchange field there are large differences, and the case of Co is in between. Interestingly, for Ni our spin-wave frequencies from the transverse susceptibility are in the high-frequency regime much larger than the experimental frequencies whereas the data from the frozen-magnon calculation agree quite well with the experimental data (apart from the experimentally observed structure at about 150 meV which results from the interference of spin waves with Stoner excitations), although the susceptibility method yields the more reliable data for the adiabatic spin

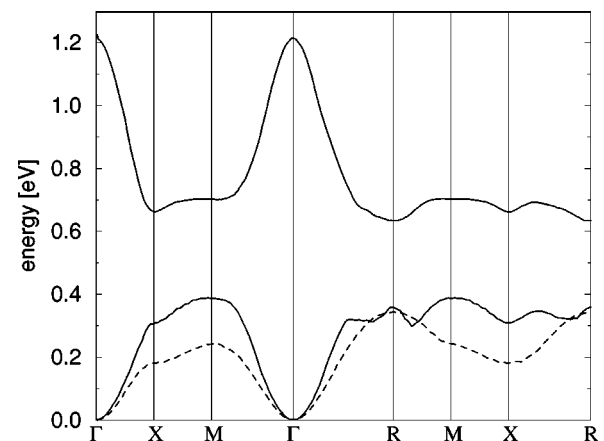


FIG. 4. Adiabatic spin-wave dispersion relations obtained by the transverse susceptibility method along high-symmetry lines of the Brillouin zone of the simple cubic elementary unit cell of Ni_3Fe (broken line) and CoFe (full line).

waves. This is related to the fact that for Ni the exchange splittings for the valence states as calculated by LSDA are a factor of about 2 larger than those obtained by photoelectron spectroscopy²¹ because the strong many-body effects in Ni cannot be accounted for by LSDA.²² The apparent success of the frozen-magnon method for Ni results from the compensation of two effects, the overestimation of the spin-wave energies in LSDA and the underestimation of the LSDA frozen-magnon frequencies because of the strong misalignment of the magnetic moments and the prescribed spin quantization axes. It should be noted that the time-dependent density-functional theory of Savrasov⁷ also yielded considerably too large magnon frequencies for Ni in the high-frequency regime.

We have also calculated the spin-wave spectra of B2-CoFe and permalloy $\text{Li}_2\text{-Ni}_3\text{Fe}$ by the transverse susceptibility method (Fig. 4), because $\text{Co}_x\text{Fe}_{1-x}$ (mainly for large x) and $\text{Ni}_x\text{Fe}_{1-x}$ (mainly for $x \approx 0.8$) are the most frequently used materials (beside Fe and Co) to study magnetoresistive effects in thin-film devices. It turned out that for Ni_3Fe the results for the three optical branches depend very critically on the detailed values of all components of the susceptibility tensor, i.e., very small changes in the k -point sampling in-

duce large changes of the frequencies. We found such a critical dependence just for this special system (not for CoFe and Ni_3Al , e.g.). Because we did not obtain really converged results for the optical branches, Fig. 4 exhibits for Ni_3Fe only the acoustical branch. Our results for the spin wave stiffness D , $500 \text{ meV}\text{\AA}^2$ for CoFe and $550 \text{ meV}\text{\AA}^2$ for Ni_3Fe can be compared with experimental data which, however, depend very sensitively on composition and sample preparation (e.g., degree of atomic order). Standing spin-wave resonance experiments on epitaxially grown $\text{Fe}_{0.55}\text{Co}_{0.45}$ films²³ and Brillouin scattering experiments on polycrystalline $\text{Fe}_{0.53}\text{Co}_{0.47}$ films²⁴ yielded $D = 360 \text{ meV}\text{\AA}^2$ and $D = (800 \pm 50) \text{ meV}\text{\AA}^2$, whereby both materials presumably were not well ordered, and a value of $D = 450\text{--}480 \text{ meV}\text{\AA}^2$ was found by inelastic neutron scattering.²⁵ Neutron-scattering experiments, magnetization experiments and spin wave resonance experiments on disordered Ni_3Fe (Ref. 26) yielded values of about $300 \text{ meV}\text{\AA}^2$, and neutron scattering experiments showed²⁷ that D increases with increasing degree of order, attaining a value of $420 \text{ meV}\text{\AA}^2$ for the best ordered samples. Altogether, we think that the agreement between theory and experiment is quite satisfactory.

¹T. Moriya, *Spin Fluctuations in Itinerant Electron Magnetism* (Springer, Berlin, 1985).

²M. Plihal and D.L. Mills, Phys. Rev. B **58**, 14 407 (1998).

³M. Plihal, D.L. Mills, and J. Kirschner, Phys. Rev. Lett. **82**, 2579 (1999).

⁴S. Zhang, P.M. Levy, A.C. Marley, and S.S.P. Parkin, Phys. Rev. Lett. **79**, 3744 (1997).

⁵M. Farle, Rep. Prog. Phys. **61**, 755 (1998).

⁶B. Hillebrands, in *Light Scattering in Solids VII*, edited by M. Cardona and G. Güntherodt (Springer, Berlin, 2000), p. 174.

⁷S.Y. Savrasov, Phys. Rev. Lett. **81**, 2570 (1998).

⁸V.P. Antropov, M.I. Katsnelson, M. van Schilfgaarde, and B.N. Harmon, Phys. Rev. Lett. **75**, 729 (1995).

⁹S.V. Halilov, H. Eschrig, A.Y. Perlov, and P.M. Oppeneer, Phys. Rev. B **58**, 293 (1998).

¹⁰Q. Niu and L. Kleinman, Phys. Rev. Lett. **80**, 2205 (1998); Q. Niu, X. Wang, L. Kleinman, W.-M. Liu, D.M.C. Nicholson, and G.M. Stocks, *ibid.* **83**, 207 (1999); R. Gebauer and S. Baroni, Phys. Rev. B **61**, R6459 (2000).

¹¹H.A. Mook and D. McK. Paul, Phys. Rev. Lett. **54**, 227 (1985).

¹²U. von Barth and L. Hedin, J. Phys. C **5**, 1629 (1972).

¹³It has been outlined in Ref. 9 that this equation holds independent of the degree of localization of $\mathbf{m}(\mathbf{r})$ as soon as the adiabatic approximation is adopted.

¹⁴P.H. Dederichs, S. Blügel, R. Zeller, and H. Akai, Phys. Rev. Lett. **53**, 2512 (1984).

¹⁵H. Köhler, J. Sticht, and J. Kübler, Physica B **172**, 79 (1991).

¹⁶L.M. Sandratskii, Adv. Phys. **47**, 91 (1998); J. Kübler, K.-H.

Höck, J. Sticht, and A.R. Williams, J. Phys. F **18**, 469 (1988).

¹⁷O. Grotheer, C. Ederer, and M. Fähnle, Phys. Rev. B **62**, 5601 (2000).

¹⁸O. Grotheer and M. Fähnle, Phys. Rev. B **59**, 13 965 (1999).

¹⁹M. Liebs, K. Hummler, and M. Fähnle, Phys. Rev. B **51**, 8664 (1995).

²⁰O.K. Andersen and O. Jepsen, Phys. Rev. Lett. **53**, 2571 (1984).

²¹W. Eberhardt and E.W. Plummer, Phys. Rev. B **21**, 3245 (1980).

²²F. Aryasetiawan, Phys. Rev. B **46**, 13 051 (1992).

²³F. Schreiber and Z. Frait, Phys. Rev. B **54**, 6473 (1996).

²⁴X. Liu, R. Sooryakumar, C.J. Gutierrez, and G.A. Prinz, J. Appl. Phys. **75**, 7021 (1994).

²⁵R.D. Lowde, M. Shimizu, M.W. Stringfellow, and B.H. Torrie, Phys. Rev. Lett. **14**, 698 (1965).

²⁶M. Hennion, B. Hennion, A. Castets, and D. Tocchetti, Solid State Commun. **17**, 899 (1975).

²⁷K. Mikke, J. Jankowska, Z. Osetek, and A. Modrzejewski, J. Phys. F **7**, L211 (1977).

²⁸G. Shirane, V.J. Minkiewicz, and R. Nathans, J. Appl. Phys. **39**, 383 (1968).

²⁹T.G. Perring, A.T. Boothroyd, D. McK. Paul, A.D. Taylor, R. Osborn, R.J. Newport, J.A. Blackman, and H.A. Mook, J. Appl. Phys. **69**, 6219 (1991).

³⁰A.T. Boothroyd, T.G. Perring, A.D. Taylor, D. McK. Paul, and H.A. Mook, J. Magn. Magn. Mater. **104-107**, 713 (1992).

³¹T.G. Perring, A.D. Taylor, and G.L. Squires, Physica B **213&214**, 348 (1995).

³²H.A. Mook and D. Tocchetti, Phys. Rev. Lett. **43**, 2029 (1979).